VIS-NIR SPECTROSCOPY OF SYNTHETIC PYROXENES: CALCIUM BEARING PYROXENES AND APPLICATION TO THE HED METEORITES. R. L. Klima[1], C. M. Pieters[1], and M. D. Dyar[2], [1]Department of Geological Sciences, Brown University, Providence RI 02912; Rachel_Klima@Brown.edu. [2]Department of Astronomy, Mount Holyoke College, South Hadley, MA 01075.

Pyroxene is one of the most common minerals in both evolved and undifferentiated solid bodies of the solar system. Pyroxene is also a particularly useful mineral because Ca exsolution, Mg-Fe order-disorder, and the chemistry of coexisting pyroxenes can be used in the laboratory to derive thermal information for pyroxene bearing rocks. Remote observations at near-infrared wavelengths detect the presence of pyroxenes on extraterrestrial surfaces with relative ease, as most pyroxene spectra are characterized by strong 1 and 2 μm absorption features. A challenge for remote sensing has been to extract quantitative mineralogical information from a pyroxene spectrum that is sufficiently robust to characterize the thermal history of remotely observed surfaces.

This study focuses on the continuing analyses of a comprehensive set of synthetic pure Ca-Fe-Mg pyroxenes to address fundamental constraints of composition and crystal structure on absorption. The relationships established in this pure system are then applied to understanding more complicated natural systems. In particular, we focus here on eucrite and diogenite meteorites, as their near-infrared spectra are dominated by pyroxene absorption features.

Background: Pyroxene spectroscopy has been the focus of a large number of studies [e.g. 1-4], including investigation into using pyroxene spectra for geothermometry [3]. Unfortunately, the textural and chemical complexity of pyroxenes has so far precluded attempts to extract geothermometric information from pyroxene absorption features [3]. Even when natural samples are well-characterized by other techniques, the number of structural and chemical variables makes linking spectral variations directly to the mineral physics extremely complicated.

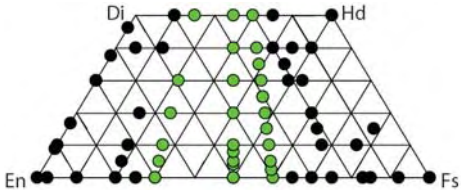

Fig. 1. Compositions available in the synthetic pyroxene series. The transects of constant Mg/Fe ratio used in this study are highlighted in green.

Approach and Preliminary Results: We are continuing a series of coordinated analyses of a set of synthetic Ca-Fe-Mg pyroxenes covering the majority of the pyroxene quadrilateral (Fig. 1), provided through the generosity of Don Lindsley and Al Turnock. This series of pyroxenes with simplified compositions offers a unique opportunity to characterize variations in near-infrared absorption bands and directly relate them to composition, crystal structure, and site preference. Results for the Ca-free orthopyroxene series have been reported previously [5,6]. We focus here on three transects of constant Mg-Fe ratio and varying Ca content (Fig. 1). The Mg-Fe ratios—Mg_{70}, Mg_{50}, and Mg_{40}—are chosen to correspond with the compositional range observed in eucrites.

The addition of Ca to a pyroxene may result in significant structural and textural variability. Though the chemical composition and P-T conditions of formation for these pyroxenes are known, we use X-ray diffraction, Mössbauer spectroscopy, and electron microprobe analyses to further characterize the synthetic pyroxenes. In particular, we are interested in determining the extent of exsolution (if present) and the ordering of Ca, Fe and Mg between the M1 and M2 crystallographic sites, an important constraint on absorption features.

The pyroxenes as synthesized consist of small crystals, often clumped together. These were sieved to <45 μm grain size and spectra were collected as bidirectional reflectance (BDR) over the wavelength range of 0.3-2.6 μm. Additional spectra were collected as diffuse reflectance and scaled and spliced to the BDR spectra to capture the full extent of the 2 μm absorption feature.

Eucrite and diogenite spectra [7] were collected similarly to the synthetic pyroxenes, but the grain sizes were somewhat more variable. In general, most meteorites were sieved to <25 μm. A pyroxene mineral separate is available for the cumulate eucrite Y-980318 [8]; other eucrite and diogenite spectra represent bulk mineralogy. We selected meteorites that were generally olivine-free, so that the near-IR spectra should represent a mixture of pyroxene and plagioclase. We further focus on meteorites in which the iron content in the plagioclase is known.

Synthetic pyroxene and HED spectra will be analyzed using the modified Gaussian model (MGM). The MGM allows a spectrum to be deconvolved into component absorption bands, which can be linked directly to the crystal field transitions in the M1 and M2 crystallographic sites [9]. We begin models with the assumption that one pyroxene is present, but add additional pyroxene bands when the RMS error indicates that they are present. When such analyses are complete, relationships between the two pyroxenes deconvolved from the spectrum and the exsolution textures of the samples will be compared.

Previous Work: Synthetic Ca-Free Pyroxenes. One of the key findings of our work on Ca-free synthetic pyroxenes is that an absorption band caused by Fe^{2+} in the M1 site is present and strong in all of the pyroxenes, even when iron content is low [5]. Previous studies using the MGM also recognized that an 1.2 μm band was needed to model natural pyroxenes, even when it was not visually obvious in a spectrum [e.g. 5,10]. This band is important for two reasons. First, the position of the pyroxene band coincides with the position of an absorption due to iron in plagioclase [11,12]. Thus, because a 1.2 μm band is present in pyroxenes, a band at that

wavelength, observed in conjunction with 1 and 2 µm pyroxene bands, cannot be assumed to represent the presence of plagioclase on a remote surface.

Secondly, comparisons between reflectance spectra and Mössbauer spectra of pyroxene show that the relative strengths of the 1.2 µm and 2 µm features are related to the proportion of iron in the M1 and M2 sites [5,13]. The primary pyroxene bands at 1 and 2 µm are caused by Fe^{2+} in the larger, more distorted M2 crystallographic site, in which Fe^{2+}generally prefers to reside in [13]. This preference is far from absolute [e.g. 14], and depends on the cooling history of the pyroxene. A relationship between the 1.2 and 2 µm bands and M1/M2 site occupancy may thus allow a qualitative assessment of pyroxene thermal history from reflectance spectra, if it is consistent over a range of pyroxene compositions.

Synthetic Ca-Bearing Pyroxenes. The addition of Ca to the pyroxene system leads to a change in crystal structure from orthorhombic to monoclinic, and alters the crystal field parameters. Saxena et al. [15] found that for low Ca (Wo_4-Wo_{20}) clinopyroxenes, the preference of Fe^{2+} for the M2 site increases with Ca content, though some portion of Fe^{2+} still enters the M1 site. We investigate the relationships between the 1.2 µm and 2 µm bands in Ca-bearing pyroxenes and those observed in the Ca-free system. We also investigate whether the relationships between the 1, 1.2 and 2 µm absorption bands observed in the Ca-free system [5] are maintained when Ca is introduced.

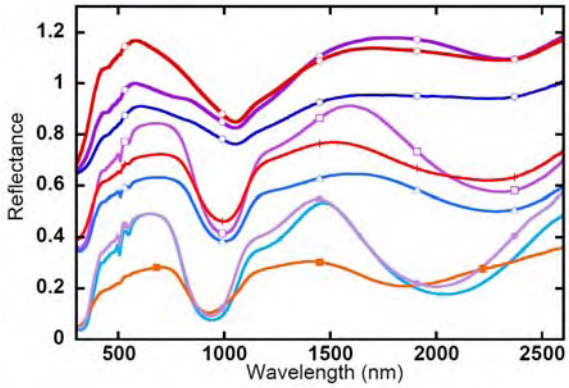

Figure 2. Selected low, medium, and high Ca synthetic pyroxene spectra from the Mg70 (reds), Mg50 (purples) and Mg40 (blues) transects. Sets of spectra are offset for clarity, with calcium increasing upwards.

Selected spectra from each of the Ca-transects are shown in Fig. 2. An absorption band is present near 1.2 µm for all synthetic samples, though the intensity as modeled by MGM for the low Ca pyroxenes is indeed weaker than the intensity of Ca-free orthopyroxenes of the same Mg/Fe ratio. Acquisition of Mössbauer spectra is in progress to quantify how this proportion compares to the ordering in the Ca-free system.

HED Meteorite Spectra. An important test is whether the relationships derived between the 1, 1.2 and 2 µm bands of synthetic pyroxenes are maintained for natural eucrite and diogenite bulk samples. Most eucrites have visually distinctive 1.2 µm features, which have been attributed both to pyroxene and to plagioclase. Shown in Fig. 3 are spectra of the bulk rock, pyroxene and plagioclase separates of the eucrite Y-980318 [8]. Unlike the spectra of lunar anorthosites, the eucrite spectrum of the plagioclase separate contains no prominent Fe^{2+} absorption features. A feature at 1.2 µm is, however, present in both the bulk and the pyroxene separate. The only immediately obvious effect of the plagioclase on the Y-980318 spectrum is an overall brightening of the spectrum. The absorption band at 1.2 µm in the bulk Y-980318 spectrum is most directly attributed to iron in the M1 pyroxene site.

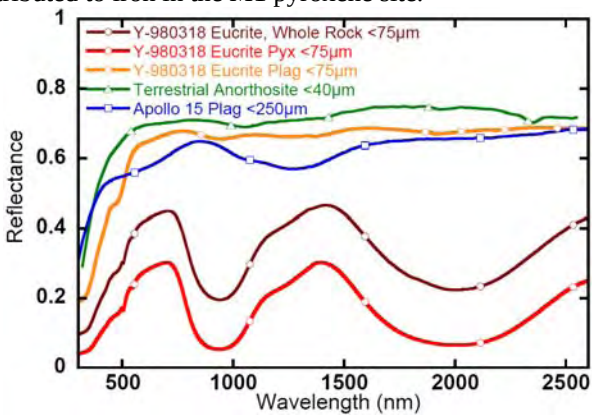

Fig. 3. Spectra of whole rock, pyroxene separate, and plagioclase separate of cumulate eucrite Y-980318 compared with anorthosite from the Moon and Earth.

We are modeling other bulk eucrite and diogenite spectra to test the hypothesis that the 1.2 µm band is caused by Fe^{2+} in the M1 site of disordered pyroxene. If strong deviations from measured relationships for pyroxene occur for meteorites with high amounts of FeO in the plagioclase, models will be tested with additional absorption bands for plagioclase. Conversely, for meteorites that have had their thermal history or site occupancy well-characterized, we will test the predicted relationships between the 1.2 and 2 µm bands derived from the thermal context. Calibration of the 1.2/2 µm band relationships for HED meteorites may allow remote characterization of whether regions of the HED parent body cooled rapidly from igneous temperatures or more slowly at depth.

Acknowledgments: Many thanks to Don Lindsley and Al Turnock for providing us with the synthetic pyroxenes. Thank you to NASA grants NNG04GG12G and NNM05AA86C (UCLA subcontract# 2090 FFC 198).

References: 1. Burns et al. (1972) *EMP 4*, 93-102. 2. Adams (1974) *JGR 79*, 4829-36. 3. Cloutis and Gaffey (1991) *JGR 96*, 22809-26. 4. Sunshine and Pieters (1993) *JGR 98*, 9075-87. 5. Klima et al. (2007) *MAPS 42*. 6. Dyar et al. (2007) *Am Min 92*, 424-8. 7. Hiroi et al. (1994) *Met 29*, 394-6. 8. Pieters et al. (2006) *Proc IAU Sym #229*, 273-288. 9. Sunshine et al. (1990) *JGR 95*, 6955-66. 10. McFadden and Cline (2005) *MAPS 40*, 151-72. 11. Bell and Mao (1973) *GCA 37*, 755-9. 12. Adams and Goullaud (1978) *LPSC IX*, 2901-9. 13. Burns et al. (1991) *NASA#N92-10823*, 253-5. 14. Saxena and Ghose (1971) *Am Min 56*, 532-559. 15. Saxena et al. (1974) *EPSL, 21*, 194-200.